Treg-mediated suppression of atherosclerosis requires MYD88 signaling in DCs

Manikandan Subramanian,[1] Edward Thorp,[2] Goran K. Hansson,[3] and Ira Tabas[1]

[1]Department of Medicine, Columbia University, New York, New York, USA. [2]Department of Pathology and Feinberg Cardiovascular Research Institute, Northwestern University, Chicago, Illinois, USA. [3]Department of Medicine, Karolinska Hospital, Stockholm, Sweden.

TLR activation on CD11c+ DCs triggers DC maturation, which is critical for T cell activation. Given the expansion of CD11c+ DCs during the progression of atherosclerosis and the key role of T cell activation in atherogenesis, we sought to understand the role of TLR signaling in CD11c+ DCs in atherosclerosis. To this end, we used a mouse model in which a key TLR adaptor involved in DC maturation, MYD88, is deleted in CD11c+ DCs. We transplanted bone marrow containing *Myd88*-deficient CD11c+ DCs into Western diet–fed LDL receptor knockout mice and found that the transplanted mice had decreased activation of effector T cells in the periphery as well as decreased infiltration of both effector T cells and Tregs in atherosclerotic lesions. Surprisingly, the net effect was an increase in atherosclerotic lesion size due to an increase in the content of myeloid-derived inflammatory cells. The mechanism involves increased lesional monocyte recruitment associated with loss of Treg-mediated suppression of MCP-1. Thus, the dominant effect of MYD88 signaling in CD11c+ DCs in the setting of atherosclerosis is to promote the development of atheroprotective Tregs. In the absence of MYD88 signaling in CD11c+ DCs, the loss of this protective Treg response trumps the loss of proatherogenic T effector cell activation.

Introduction

In atherosclerosis, the subendothelial retention and modification of apolipoprotein B–containing lipoproteins drives a chronic inflammatory response characterized by activation of both the innate and adaptive arms of the immune system (1). This inflammatory response contributes to the expansion of the atherosclerotic plaque and eventually to the creation of necrotic lesions capable of triggering acute atherothrombotic cardiovascular events (2). A major component of the innate response involves the entry of monocytes into nascent lesions, followed by differentiation of monocytes into macrophages and CD11c+ cells with DC-like properties (3). Lesional monocyte-derived DCs, and possibly conventional DCs, can link innate and adaptive immunity, because, upon exposure to TLR ligands, DCs mature and present antigen to and activate naive T cells. T cell activation is further promoted by the production of T cell–activating cytokines, such as IL-12, by the TLR-activated DCs (4).

Different classes of T cells have different effects on atherogenesis (5). For example, studies in mice have provided evidence that Th1 cells are atherogenic (6), while Th2 cells and Tregs are atheroprotective (5, 7); the role of Th17 is still unclear (8, 9). Thus, the net effect of DC-mediated T cell activation on atherogenesis would depend on the type(s) of T cells that is activated in the environmental and antigen context of atherosclerosis. Most mouse studies in which DCs have been depleted or disabled show a decrease in atherosclerosis, suggesting that a major role of DCs is activation of proatherogenic T effector (Teff) cells (10–13). On the other hand, a recent study showed that deletion of Flt3, which results in defective development of conventional DCs, a decrease in lesional CD103+ DCs, and a systemic decrease in Tregs, is associated with an increase in atherosclerosis (14). While these studies have provided important information in this new area of research, major gaps in our understanding of the role of DCs in atherosclerosis remain. Most

notably, we have only very limited information on the molecular and cellular mechanisms by which DC manipulations affect specific atherogenic processes. Filling in these gaps of knowledge is not only important for furthering our understanding of the role of the immune system in atherogenesis but also has direct implications for new "DC-vaccine" strategies that take advantage of DC-mediated Treg activation to suppress atherogenesis (15, 16).

In this context, we present the results of a study using what we believe to be a new, global approach to interrogate the role of CD11c+ antigen-presenting cells in atherosclerosis. Using a bone marrow transplantation strategy, we reconstituted atherosclerosis-prone *Ldlr*^{−/−} mice with marrow isolated from *Cd11c-Cre+Myd88*^{fl/fl} (Cre+) mice. In these mice, CD11c+ cells lack the TLR adaptor MyD88, which decreases their ability to activate Teff cells (17). Contrary to what might have been predicted (18), these mice show a surprising *increase* in lesion size and monocyte infiltration. The mechanism of increased atherosclerosis in the mutant mice involves suppression of Tregs, leading to an increase in the monocyte chemoattractant, MCP-1. These data establish that the dominant role of mature CD11c+ DCs in atherosclerosis is the promotion of Treg development, which in turn suppresses the monocyte inflammatory response.

Results

CD11c-MyD88 deficiency suppresses DC maturation and T cell activation under hypercholesterolemic conditions. We first validated the usefulness of the model in suppressing DC maturation in a non-atherosclerosis setting. Cre+ mice or control *Cd11cCre−Myd88*^{fl/fl} (Cre−) mice were injected with the TLR9 activator CpG, and splenic CD11c+ cells were analyzed for signs of DC maturation. We found a significant decrease in the expression levels of DC maturation markers CD86 and CD40 in the cells from Cre+ mice, consistent with defective DC maturation (Supplemental Figure 1; supplemental material available online with this article; doi:10.1172/JCI64617DS1). To study the effect of CD11c-targeted MyD88 deletion in a model of LDL-driven atherosclerosis, we trans-
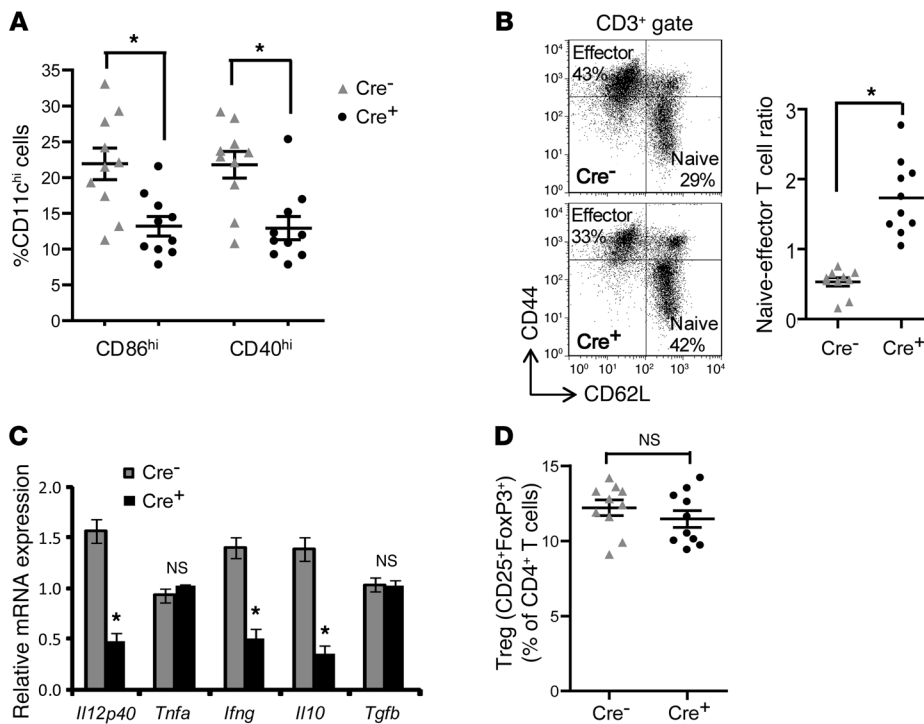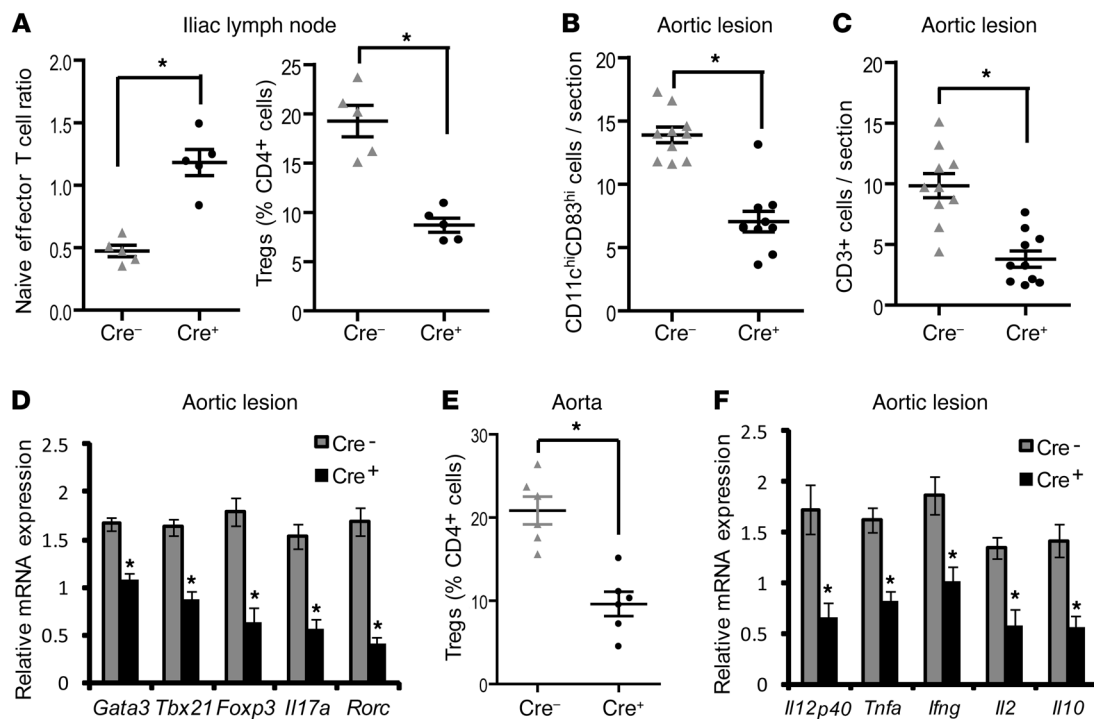
Figure 1

Maturation of splenic DCs is inhibited in WD-fed *Ldlr*^{−/−} mice transplanted with bone marrow from Cre+ mice. For this figure and the following 5 figures, *Ldlr*^{−/−} mice transplanted with Cre− or Cre+ bone marrow were fed WD for 10 weeks. For the data here, *n* = 10 mice per group unless otherwise indicated. (**A**) Percentage of CD11c^{hi} DCs expressing the DC maturation marker CD86 or CD40 in the spleens of Cre− or Cre+ mice. (**B**) Representative flow cytometric dot plots of CD3+-gated splenocytes, demonstrating the distribution of naive (CD62L^{hi}CD44^{lo}) and effector T cells (CD62L^{lo}CD44^{hi}) in Cre− and Cre+ mice. The scatter plot shows the quantification of the splenic naive/effector T cell ratio. (**C**) The indicated cytokine mRNA levels were determined by RT-qPCR analysis of RNA isolated from the spleens of Cre− or Cre+ mice (*n* = 5 mice per group). All data were normalized to the expression of *Gapdh*. (**D**) Flow cytometric quantification of Treg numbers in the spleens of Cre− and Cre+ mice, expressed as a percentage of total CD4+ T cells. For all panels, *$P < 0.05$. n.s., not significant. Symbols represent individual mice; horizontal bars indicate the mean.

planted bone marrow from Cre+ or Cre− mice into lethally irradiated male *Ldlr*^{−/−} mice, and 6 weeks later the mice were placed on an atherogenic Western-type diet (WD) for 10 weeks. As in the CpG model, the Cre+-transplanted *Ldlr*^{−/−} mice showed a significant decrease in the percentage of splenic CD11c+ cells expressing CD86 and CD40 (Figure 1A and Supplemental Figure 2, A–C). No significant difference was observed between the 2 groups of mice in the percentage distribution of CD11c+, F4/80+, or CD3+ cells in the spleen (Supplemental Figure 2D), suggesting that MyD88 deletion in CD11c+ cells does not alter the relative distribution of DCs, macrophages, or T cells in the spleen. Since DC maturation and antigen presentation result in the differentiation of naive T cells to effector/memory T cells, we measured the relative distribution of naive and effector T cells in the spleens of these mice. Consistent with suppression of DC maturation in the Cre+ mice, there was a significant increase in the numbers of naive T cells, as reflected by the increase in the naive/effector T cell ratio in the spleen (Figure 1B). As a further confirmation of suppression of DC maturation, we measured the mRNA of cytokines expressed by mature DCs and activated T cells and found a significant decrease in the levels of *Il12*, *Il10*, and *Ifng* mRNA in the Cre+ mice (Figure

1C). In contrast, there was no significant difference in *Tgfb* mRNA or the percentage of Tregs in the spleens of Cre+-transplanted *Ldlr*^{−/−} mice (Figure 1, C and D). These data demonstrate that deletion of MyD88 in CD11c cells suppresses splenic DC maturation and Teff cell activation in the setting of hypercholesterolemia.

One hypothesis for the presence of activated T cells in atherosclerotic lesions is DC-mediated presentation of antigens to T cells in peripheral lymph nodes and perhaps the lesions themselves (5, 19). As shown in Figure 2A, analysis of aorta-draining iliac lymph nodes demonstrated that the naive/effector T cell ratio was significantly higher in the Cre+ mice and the percentage of Tregs was lower, while the total T cell numbers were unaffected (data not shown). We next determined whether DC maturation and T cell activation were suppressed in the atherosclerotic lesions of the Cre+ mice. Note that the CD11c^{hi} regions, but not the CD11c^{lo} regions, showed a loss of *Myd88* mRNA (Supplemental Figure 3B). As in the spleen, there was a significant decrease in the number of CD11c^{hi} cells expressing the DC maturation marker CD83 in the aortic root lesions of Cre+ mice, indicating suppression of DC maturation within the atherosclerotic plaque (Figure 2B and Supplemental Figure 4). We next compared total CD3+ T cells, T cell subsets based on their unique mRNA signatures, and

mRNA levels of T cell–derived cytokines in the aortic root lesions of Cre− and Cre+ *Ldlr*^{−/−} mice fed the Western diet for 10 weeks. Cre+ lesions were found to have a striking decrease in total CD3+ cells (Supplemental Figure 12) as well as decreases in the major T cell subsets, namely, Th1 (*Tbx21*, also known as *Tbet*) and Th17 (*Rorc*) cells, which have been shown in several studies to promote atherosclerosis, and Th2 (*Gata3*) and Treg (*Foxp3*) cells, which are thought to be atheroprotective (Figure 2, C and D). We further confirmed by flow cytometric analysis of aortic cells that the percentage of aortic Tregs (CD4+CD25+FoxP3+) was decreased in the Cre+ mice (Figure 2E). Consistent with this finding, the mRNA for cytokines secreted by these cells or that maintain them, including *Il12*, *Tnfa*, *Ifng*, *Il2*, and *Il10*, was also suppressed in the Cre+ lesions (Figure 2F). Note that CD3+ cells sorted by FACS from the Cre− and Cre+ lesions showed identical expression of *Myd88* mRNA (Supplemental Figure 5), indicating that these findings were not due to MyD88 deficiency in the T cells themselves. Consistent with these in vivo findings, in vitro culture of ovalbumin-specific (ova-specific) OT-II naive T cells with ova-loaded mature Cre+ bone marrow–derived DCs revealed deficient Teff cell and Treg generation (Supplemental Figure 6). Moreover, the defect in Teff cell and

Figure 2
Lesional T cells are decreased in WD-fed $Ldlr^{-/-}$ mice transplanted with bone marrow from Cre+ mice. (**A**) Naive (CD62L^{hi}CD44^{lo})/effector (CD62L^{lo} CD44^{hi}) T cell ratio and percentage of Tregs (CD4+CD25+FoxP3+), as determined by flow cytometry in the iliac lymph nodes of Cre− and Cre+ mice (n = 5 mice per group). (**B** and **C**) Number of CD11c^{hi}CD83^{hi} cells and CD3+ cells per section in the atherosclerotic lesions of Cre− and Cre+ mice, as determined by quantitative immunofluorescence microscopy (n = 10 mice per group). (**D** and **F**) The indicated mRNA levels were determined by RT-qPCR analysis of RNA captured from CD11c^{lo} regions of the plaques of Cre− and Cre+ mice (n = 5 mice per group). The data were normalized to *Gapdh* mRNA expression. (**E**) Flow cytometric quantification of Tregs (CD4+CD25+FoxP3+) expressed as a percentage of total CD4+ cells obtained from aortic extracts of Cre− and Cre+ mice. The recovery efficiency of aortic leukocytes was >80% (n = 5 mice for Cre− and 6 mice for Cre+). For all panels, *P < 0.05. Symbols represent individual mice; horizontal bars indicate the mean.

Treg development could be rescued by exogenous costimulation of T cells with anti-CD28 antibody treatment, which is consistent with the defect being due to defective maturation-dependent costimulation by Cre+ DCs.

CD11c-MyD88 deficiency promotes atherosclerosis and lesional accumulation of myeloid-derived cells. The CD11c-MyD88–deficient model presents a unique opportunity to assess the net effect of DC-mediated T cell activation on atherogenesis, particularly given that the lesional T cell and cytokine profile is altered in a manner that could either suppress or promote atherogenesis. Despite a number of previous studies implicating a proatherogenic role for DC-mediated T cell activation (11, 12, 20–22), CD11c-targeted MyD88 deletion led to an increase in aortic root cross-sectional lesion area and in en face Oil red O–positive area in the thoracic aorta (Figure 3, A and B). Note that there were no significant differences in the plasma cholesterol, triglyceride, and levels of VLDL, LDL, and HDL cholesterol between the 2 groups of mice (Figure 3, C–E), indicating that the larger lesions in the Cre+ mice cannot be explained by alterations in plasma lipoprotein levels. To address whether the increase in lesion area was due to increased cellularity of the lesions, we quantified the number of CD11c^{lo}F4/80+ cells (macrophages), CD11c^{hi} cells (DCs), and smooth muscle cells. The data show a significant increase in the numbers of both macrophages and DCs in the Cre+ lesions, while the smooth cells were unaffected (Figure 3F).

Because plaque macrophages and the majority of plaque DCs are derived from circulating monocyte precursors (14), we wondered whether the increased cellularity was due to enhanced monocyte recruitment into the lesions of Cre+ mice. To test this possibility, we used a previously described method of labeling monocytes with fluorescent beads and then tracked their appearance in atherosclerotic lesions (23). We first confirmed that the bead labeling efficiency of blood monocytes was similar between the 2 groups of mice (data not shown). Analysis of lesions by fluorescence microscopy revealed a significant increase in the number of bead-labeled cells in Cre+ lesions compared with that in Cre− lesions, suggesting increased monocyte recruitment (Figure 4A). This finding was not associated with a difference in the peripheral blood monocyte count or an alteration in the relative distribution of Ly6C^{hi} and Ly6C^{lo} monocyte subsets (Figure 4, B and C). Moreover, there was no significant difference in the endothelial expression of two key monocyte adhesion molecules, VCAM-1 and *Cx3cr1* (Supplemental Figure 7, A and B). There was also no change in the expression level of *Cx3cl1* (Supplemental Figure 7C), the ligand for CX3CR1, which was shown previously to enhance monocyte recruitment in atherosclerosis (24). However, there was a striking increase in the level of *MCP1* mRNA in both CD11c^{hi} and CD11c^{lo} regions, demonstrating that this key monocyte chemokine is increased in both DCs and macrophages in Cre+ lesions (Figure 4D). Moreover,
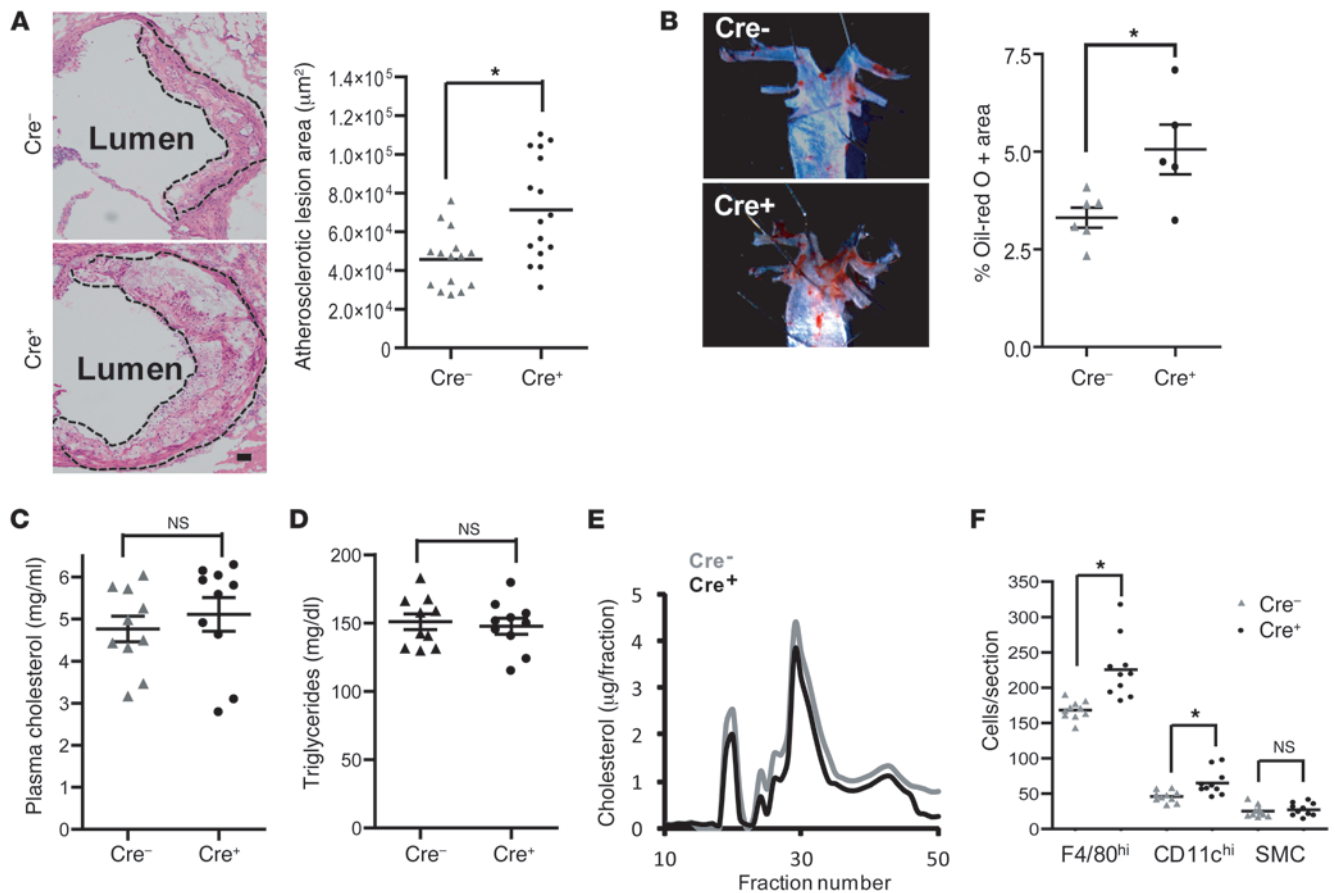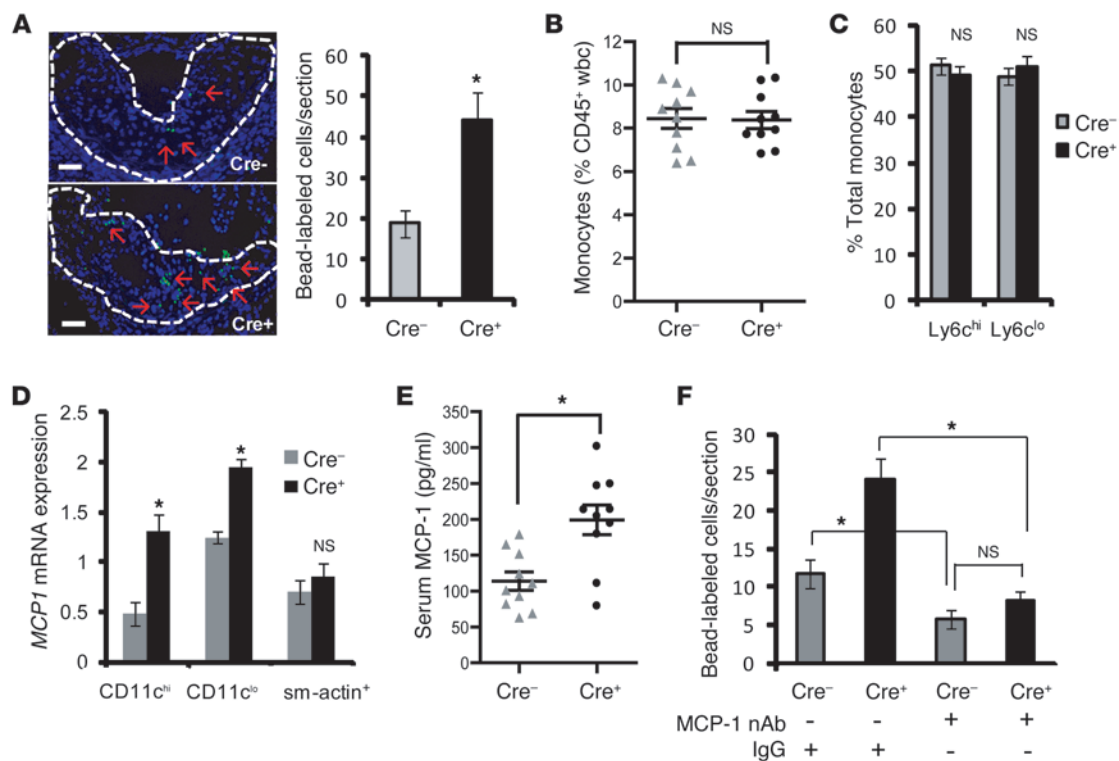
Figure 3
Atherosclerosis is increased in WD-fed *Ldlr$^{-/-}$* mice transplanted with bone marrow from Cre$^+$ mice. (**A**) H&E staining of representative aortic root sections demonstrating larger lesion size in *Ldlr$^{-/-}$* mice transplanted with bone marrow from Cre$^+$ mice. The atherosclerotic lesions are demarcated by the dashed lines. Scale bar: 10 μm. The scatter plot shows the quantified data from 15 Cre$^-$ and 16 Cre$^+$ mice. (**B**) Representative images of Oil red O–stained thoracic aorta showing lesional area in Cre$^-$ and Cre$^+$ mice. The scatter plot shows the quantified data from 6 Cre$^-$ and 5 Cre$^+$ mice. (**C** and **D**) Plasma cholesterol and total triglycerides in Cre$^-$ and Cre$^+$ mice, respectively. (**E**) Distribution of VLDL, LDL, and HDL cholesterol by fast performance liquid chromatography of pooled plasma samples. (**F**) Number of CD11c$^-$F4/80$^+$ (macrophages), CD11c^{hi} (DCs), and smooth muscle (sm-actin$^+$) cells (SMCs) per section in the atherosclerotic lesions of Cre$^-$ and Cre$^+$ mice, as determined by quantitative immunofluorescence microscopy (*n* = 10 mice per group). For all panels, *$P < 0.05$. Symbols represent individual mice; horizontal bars indicate the mean.

the concentration of MCP-1 was significantly higher in the serum of Cre$^+$ mice (Figure 4E). To assess the causal relationship between the elevation of MCP-1 and lesional monocyte entry in Cre$^+$ mice, the 2 groups of mice were injected with a neutralizing antibody against MCP-1. As shown in Figure 4F, neutralization of MCP-1 blocked monocyte entry in the Cre$^+$ mice to a level equivalent to that seen in the Cre$^-$ mice. Thus, disruption of T cell activation in Cre$^+$ mice has a net proatherogenic effect that is caused by an increase in MCP-1–induced monocyte entry into lesions.

Tregs decrease monocyte recruitment into lesions via suppression of MCP-1. Treg numbers, which are lower in the lymph nodes and lesions of Cre$^+$ mice, have a suppressive effect on proinflammatory mediators released by myeloid cells (25). We therefore hypothesized that the increase in *MCP1* in the atherosclerotic lesions of Cre$^+$ mice was due to a loss of Treg-mediated suppression of this inflammatory process. To test this hypothesis, we depleted Tregs in WD-fed Cre$^-$ *Ldlr$^{-/-}$* mice to determine whether this could mimic the increase in *MCP1* mRNA and monocyte recruitment seen in

the Cre$^+$ mice. Partial Treg depletion was accomplished using anti-CD25 antibody (7, 26) 2 weeks prior to the completion of the 10-week WD feeding period. To validate the method, we show that antibody treatment resulted in approximately 75% depletion of Tregs in the spleen (Supplemental Figure 8) and approximately 65% decrease in lesional *Foxp3* mRNA, while lesional *Tbx21* mRNA, a marker of Th1 cells, was not decreased (Figure 5A). Moreover, Tregs are a major source of TGF-β (25), and lesional *Tgfb* mRNA was also lower in the anti-CD25–treated mice. As predicted by the hypothesis, the lesions of antibody-treated mice had an increase in lesional *MCP1* mRNA and an increase in monocyte recruitment into the lesions (Figure 5B).

We then conducted the converse experiment to determine whether adoptive transfer of Tregs could block the increase in *MCP1* and monocyte recruitment in Cre$^+$ mice. Based on previous studies showing that transfered natural Tregs (nTregs) isolated from the spleen could traffic to specific inflammatory sites (27), splenic Tregs were isolated from CD45.1 C57BL/6J WT mice

Figure 4
Recruitment of monocytes into atherosclerotic lesions is enhanced in WD-fed *Ldlr*$^{-/-}$ mice transplanted with bone marrow from Cre$^+$ mice through an MCP-1 mechanism. (**A**) Representative images demonstrating increased fluorescent bead-labeled monocytes (green staining, indicated by red arrows) in atherosclerotic lesions of Cre$^+$ mice. Nuclei are stained with Hoechst 33342 (blue). Scale bar: 10 μm. The bar graph shows quantification of the number of labeled cells per section in aortic root lesions of Cre$^-$ (*n* = 4) and Cre$^+$ (*n* = 5) mice. (**B**) Peripheral blood monocytes were quantified by CD115 staining using flow cytometry and expressed as a percentage of CD45$^+$ leukocytes (*n* = 10 mice per group). (**C**) Flow cytometric analysis of distribution of Ly6C^{hi} and Ly6C^{lo} monocyte subsets of CD45$^+$CD115$^+$-gated leukocytes (monocytes). (**D**) Quantification of *MCP1* mRNA in RNA isolated from CD11c^{hi}, CD11c^{lo}, and smooth muscle actin (sm-actin$^+$) regions of atherosclerotic lesions of Cre$^-$ and Cre$^+$ mice. The data were normalized to expression of *Gapdh* (*n* = 5 mice per group). (**E**) Measurement of serum MCP-1 levels by ELISA in Cre$^-$ and Cre$^+$ mice (*n* = 10 mice per group). (**F**) Fluorescence microscopy-based quantification of the number of bead-labeled cells per lesion section of Cre$^-$ or Cre$^+$ mice injected with IgG or MCP-1–neutralizing antibody (MCP-1 nAb) on days 1, 3, and 8 prior to the end of the WD-feeding period. For all panels, *P < 0.05. Symbols represent individual mice; horizontal bars indicate the mean.

(Supplemental Figure 9A) and injected into WD-fed CD45.2 Cre$^+$ *Ldlr*$^{-/-}$ mice. CD45.1$^+$ cells were detected within the atherosclerotic lesions as well as in the adjoining adventitia in mice adoptively transferred with Tregs (Supplemental Figure 9B). Most importantly, there was a significant increase in the expression level of *Foxp3* and *Tgfb*, and, as predicted by the hypothesis, a decrease in *MCP1* mRNA (Figure 5C) and monocyte recruitment (Figure 5D).

Previous in vitro studies have demonstrated that LPS-induced MCP-1 secretion by macrophages is suppressed by TGF-β through Smad3-dependent inhibition of AP-1 binding to the *MCP1* promoter (28, 29). Thus, one possible mechanism for the decrease in lesional *MCP1* in the Cre$^+$ lesions could be defective TGF-β–mediated suppression of *MCP1*. Although causation studies to test this hypothesis will require a future project combining the models in this study with those having defective TGF-β action, we sought to determine here whether TGF-β action might be defective in Cre$^+$ lesions. Indeed, *Tgfb* mRNA was substantially lower in DC-rich (CD11c^{hi}), macrophage-rich (CD11c^{lo}), and smooth muscle cell–rich (sm-actin$^+$) regions of atherosclerotic lesions of Cre$^+$ mice (Figure 6A). This result, combined with the previous

data from the Treg models (Figure 5), suggests that Tregs and/or other cells stimulated by Tregs are the major cellular source of TGF-β in lesions. Consistent with the mRNA data, TGF-β protein levels in the lesional extract were significantly lower in the Cre$^+$ lesions (Figure 6B). The activity of TGF-β is tightly controlled by several processes, including its secretion, as well as cleavage from latency-associated peptide, which maintains TGF-β in an inactive form (30). The data in Figure 6B are for latent TGF-β, while the activated form was below the limit of detection of the ELISA assay. This finding is consistent with previous studies demonstrating difficulty in measuring the active form in vivo, presumably due to its low levels or short half-life (31). We therefore tested the "bioactivity" of TGF-β in lesions by assaying the expression of 3 TGF-β–responsive smooth muscle cell genes, *Col1a1*, *Col3a1*, and *Egr1*, in sm-actin$^+$ regions of the lesions. The mRNA levels of all 3 genes were significantly decreased in the lesions of Cre$^+$ mice (Figure 6C). Thus, Cre$^+$ lesions have diminished TGF-β mRNA, protein, and target gene expression. Furthermore, blocking TGF-β action in WD-fed *Ldlr*$^{-/-}$ mice by injecting an anti–TGF-β neutralizing antibody resulted in significant upregulation of *MCP1* mRNA in
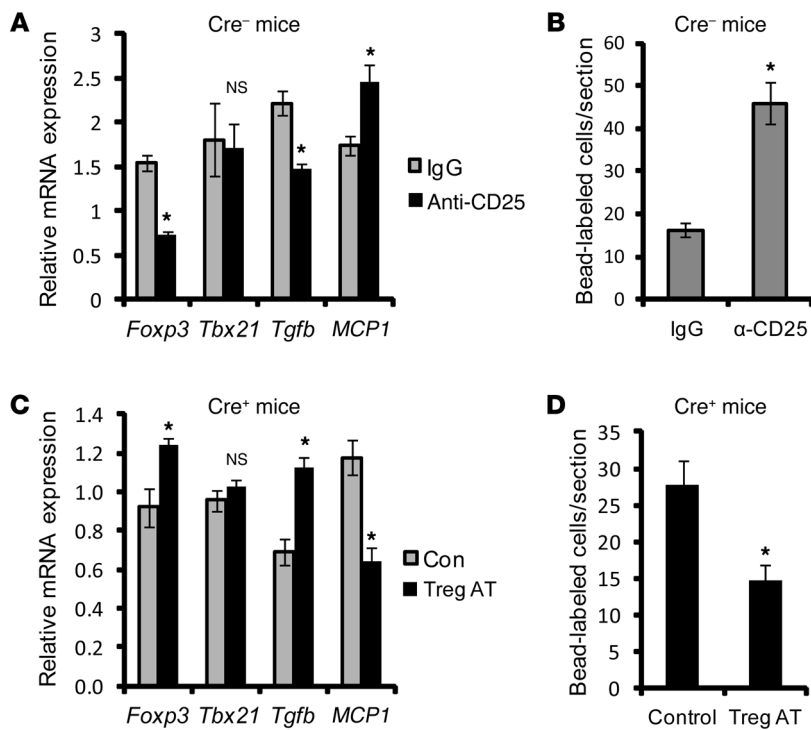
Figure 5

Evidence that MyD88 deficiency in CD11c⁺ cells abrogates Treg-mediated suppression of MCP-1 and monocyte recruitment in the lesions of WD-fed *Ldlr*⁻/⁻ mice. (**A**) WD-fed *Ldlr*⁻/⁻ mice transplanted with bone marrow from Cre⁻ mice were injected with anti-CD25 IgG to deplete Tregs or with control IgG. Two weeks later, the mRNA levels of the indicated targets were assayed in LCM-captured RNA obtained from CD11c^lo regions of atherosclerotic lesions. The data were normalized to the expression level of *Gapdh* mRNA ($n = 5$ mice per group). (**B**) Quantification of the number of fluorescent bead-labeled cells per section in control and Treg-depleted Cre⁻ mice ($n = 3$ mice per group). (**C** and **D**) Tregs were adoptively transferred into WD-fed *Ldlr*⁻/⁻ mice transplanted with bone marrow from Cre⁺ mice (Treg AT); as a control (Con), the mice were injected with the Treg vehicle. Two weeks later, lesions were quantified for the indicated mRNA levels ($n = 5$) and for bead-labeled monocytes as above ($n = 3$). For all panels, $*P < 0.05$.

the extracts obtained from the intima of atherosclerotic lesions of these mice (Figure 6D). This result, combined with the decrease in TGF-β in the Cre⁺ lesions and the aforementioned *MCP1* gene regulation studies (28, 29), provides a plausible explanation for the increase in lesional *MCP1* expression and monocyte recruitment in the lesions of Cre⁺ mice.
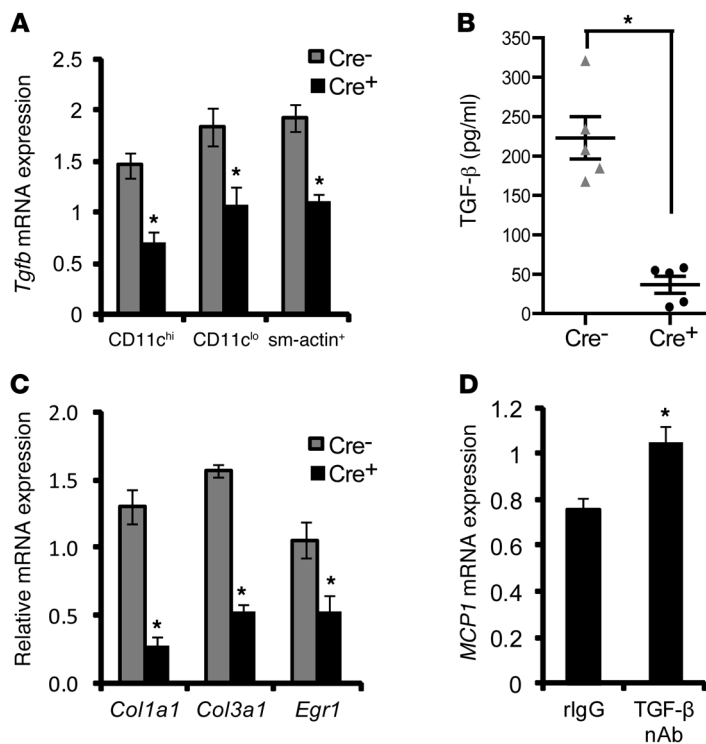
Discussion

In the context that atherogenesis is driven by a chronic, maladaptive inflammatory response, the identification of DCs in the atherosclerotic plaques of humans (32–34) and mice (3, 10, 11, 14, 20–22, 35) has been of tremendous interest due to the potent antigen-presenting capacity of DCs and their ability to activate T cells. However, different T cell subsets can either promote or suppress atherogenesis, and thus the net effect of DC-mediated T cell activation in the setting of atherosclerosis is perhaps the most important question in this critical area of research. In this study, we show that, although MyD88-mediated maturation of CD11c⁺ DCs is necessary for the full activation of both Teff cells and Tregs in lesions and lymph nodes, the net effect is Treg-mediated suppression of atherogenesis (Figure 7). The mechanisms involve the expected effects of Tregs in terms of suppression of proinflammatory Teff cells and macrophages, but we also reveal another key mechanism in which Treg-induced TGF-β suppresses MCP-1. In that regard, the data support an important and fundamental concept, namely, that the well-known role of Tregs in adaptive immunity, i.e., through suppression of T cell activation, is complemented by an innate immune function involving suppression of monocyte/macrophage influx and activation.

A number of previous studies have used various manipulations to perturb DC function in mouse models of atherosclerosis. In a few of these studies, direct effects on atherogenesis could not be discerned because the manipulations affected plasma cholesterol levels (10), which was not the case in the *Cre*⁺ model used here.

Other studies restricted monocyte entry using CX3CR1-deficient mice (21) or inhibited monocyte differentiation into DCs using GM-CSF–deficient mice (11) or restricted DC egress from lesions using CCR7-deficient mice (36). In all these mouse models, atherosclerosis was deceased, not increased as in the *Cre*⁺ model, suggesting a proatherogenic role for DCs. However, deletion of CX3CR1, GM-CSF, or CCR7 suppresses other processes that influence atherosclerosis, such as monocyte recruitment (3), inflammation (37), and T cell trafficking (36), respectively.

Previous reports have indicated that MyD88 signaling in macrophages is proatherogenic (38, 39). Thus, deletion of MyD88 in CD11c-expressing macrophages in atherosclerotic lesions (13) could potentially decrease lesional inflammation and thus suppress atherosclerosis. If this were the case, the data herein would indicate that the proatherogenic effects of MyD88 depletion in CD11c⁺ DCs are dominant over the potentially antiatherogenic effects of MyD88 depletion in CD11c⁺ macrophages. Although distinctions between DCs and macrophages based on cell-surface markers are difficult to make due to the pleiotropic nature of the markers used and monocyte plasticity (3, 40–42), we found that lesional CD11c^hi cells had a cytokine profile more similar to that of splenic DCs than to that of splenic macrophages (data not shown). Moreover, the clearance of lesional apoptotic cells (efferocytosis) by CD11c^hi cells in plaques was not affected by deletion of MerTK, which is an efferocytosis receptor used by macrophages, including lesional macrophages, but not by DCs (43, 44) (data not shown). In the end, the key issue is the functional attributes of monocyte-derived cells, which in the context of this study is the ability of CD11c⁺ cells to alter the T cell profile of atherosclerotic lesions through MyD88-dependent antigen presentation and cytokine production.

Various models have provided evidence that nTregs and those induced by exogenous antigen treatment are atheroprotective (7, 14, 22, 45–48). As a proof-of-concept restoration experiment, we

Figure 6
Evidence of a link between decreased TGF-β and increased *MCP1* in lesions of WD-fed *Ldlr*⁻/⁻ mice transplanted with bone marrow from Cre⁺ mice. (**A**) LCM RT-qPCR analysis of *Tgfb* mRNA in RNA obtained from CD11cʰⁱ, CD11cˡᵒ, and sm-actin⁺ regions of atherosclerotic lesions of Cre⁻ and Cre⁺ mice (n = 5 mice per group). (**B**) ELISA-based measurement of latent TGF-β from extracts of atherosclerotic lesions of Cre⁻ and Cre⁺ mice (n = 5 mice per group). (**C**) *Col1a1*, *Col3a1*, and *Egr1* mRNA in RNA obtained from sm-actin⁺ regions of atherosclerotic lesions of Cre⁻ and Cre⁺ mice (n = 5 mice per group). (**D**) Analysis of *MCP1* mRNA expression in RNA obtained from the intima of atherosclerotic lesions of 10-week WD-fed *Ldlr*⁻/⁻ mice treated with rat IgG (rIgG) or a neutralizing rat IgG antibody against TGF-β (TGF-β nAb) (100 μg per mouse) on days 1, 3, and 8 prior to sacrifice. The data were normalized to expression of *Gapdh* (n = 6 mice per group). For all panels, *$P < 0.05$. Symbols represent individual mice; horizontal bars indicate the mean.

showed that adoptive transfer with nTregs can reverse the MCP-1/monocyte phenotype of the Cre⁺ mice. Whether nTregs are more or less important than "inducible" Tregs (iTregs) in the *endogenous* setting of atherosclerosis is not known. However, our finding that blocking DC maturation leads to a functionally important Treg defect in the endogenous setting of atherosclerosis might possibly suggest a role for iTregs activated by endogenously stimulated DCs. This possibility is based on the finding that DC-mediated activation of nTregs requires much less antigen than DC-mediated induction of iTregs from naive T cells, which has led to the suggestion that nTreg activation is not as dependent on DC maturation as induction of Tregs from naive T cells (49, 50). Consistent with this possibility, splenic nTregs were not altered in the Cre⁺ model. In the end, it is difficult to distinguish nTregs from iTregs (51), and future studies will be needed to determine whether there are endogenous antigen(s) that might be involved. Previous studies using *exogenous* antigens have suggested that two proteins found in atherosclerotic lesions, apolipoprotein B-100 (16) and Hsp60 (45, 48), might be involved in Treg activation, but evidence in the endogenous situation is lacking.

This study is also distinguished by its identification of a specific mechanism that links DC-mediated Treg activation with protection from atherosclerosis. Tregs have the ability to suppress Teff cell activation as well as exert inhibitory action on macrophages, DCs, and vascular endothelial cells by either direct cell-cell contact or by secreting effector cytokines such as TGF-β and IL-10 (52, 53). As depicted in Figure 7, our data support a model in which DC-mediated Treg activation suppresses monocyte recruitment via decreasing the levels of monocyte chemokine MCP-1, probably in a TGF-β–dependent manner. Moreover, Treg-induced TGF-β may further enhance the antiinflammatory and antiatherosclerotic response through direct actions of TGF-β on DCs themselves (54). IL-10, another major Treg-secreted atheroprotective cytokine (55), was

lower in both the spleens and lesions of the Cre⁺ mice. However, Treg depletion and adoptive transfer of Tregs, which are associated with changes in *MCP1* mRNA levels, did not show significant changes in *Il10* mRNA expression (Supplemental Figure 10), suggesting that IL-10 does not directly regulate MCP-1 expression in lesions.

This study raises a number of intriguing questions for future studies. For example, is DC-mediated T cell activation occurring in draining lymph nodes, followed by T cell homing to lesions, or might there also be DC/T cell activation occurring in the lesions themselves? A recent study demonstrated productive interaction of CD4⁺ T cells with CD11cʰⁱ cells in the vascular wall of atherosclerotic lesions ex vivo, suggesting that lesional CD11cʰⁱ DCs could activate T cells in the atherosclerotic lesions in vivo (19). In this context, we observed decreased Treg numbers not only in aorta-draining iliac and mediastinal lymph nodes of Cre⁺ mice, but also in the nondraining inguinal lymph nodes (Supplemental Figure 11). These data raise the interesting possibility that systemically circulating antigens such as oxidized lipids may also be involved in activating the adaptive immune system in atherosclerosis. Another question that warrants further investigation is how MyD88 signaling in DCs affects advanced atherosclerosis progression, because deficient MyD88 signaling in CD11cʰⁱ cells was associated with a decrease in procollagen mRNA synthesis (Figure 6C) as well as a decrease in intimal collagen content (data not shown), which can be a marker of plaque stability when observed in human atheromata (56). In this regard, immunoneutralization of TGF-β in *Apoe*⁻/⁻ mice was shown to promote the development of collagen-poor advanced plaques (57).

In summary, we have provided evidence that endogenous MyD88-mediated DC activation and maturation is atheroprotective through the generation of Tregs. The findings provide new insight into how the critical crossroads of adaptive and innate immunity affect atherosclerosis. Moreover, the insight gained
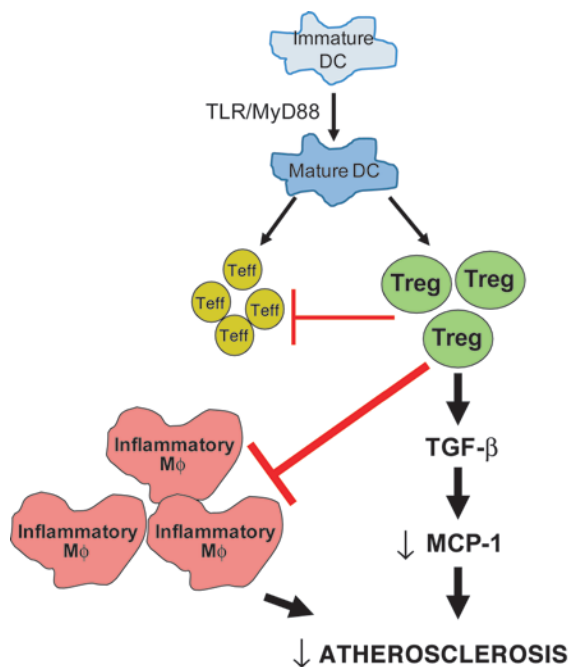
Figure 7
Schematic showing the mechanism of atheroprotective action of Tregs. In atherosclerosis, mature DCs activate both Teff cells and Tregs. This study suggests that the atheroprotective effect of Tregs dominates. Tregs exert their atheroprotective action via suppression of Teff cells and inflammatory macrophages (Mφs), and they suppress monocyte recruitment by decreasing MCP-1 production in a TGF-β–dependent manner.

En face Oil red O staining and analysis. The thoracic aorta was dissected from the heart and surrounding tissues and the adventitial fat tissue was cleaned and incubated overnight in 10%-buffered formalin. The aorta was then splayed open longitudinally under a dissecting microscope and pinned to silicone-coated plates, and Oil red O staining was performed. Images were acquired, and Oil red O–positive area was analyzed by applying a color threshold in Adobe Photoshop.

Immunochemistry, flow cytometry, and microscopy. Subcellular analysis of peripheral blood wbc, splenocytes, and lymph node cells was performed by immunochemistry using fluorophore-conjugated primary antibodies against CD4, CD25, CD115, and FoxP3 (all from eBioscience) and Ly6C/G, CD11c, F4/80, CD3, CD62L, CD44, CD40, CD83, CD86, and MHC II (all from BD Biosciences). The samples were analyzed on a FACSCalibur flow cytometer equipped with a 488-nm and a 543-nm laser. Immunohistochemistry on aortic root sections was performed by fixing the frozen sections in ice-cold acetone and then labeling with unconjugated primary antibodies against CD11c, F4/80, and CD3 (all from BD Biosciences); VCAM-1 (R&D Systems); sm-actin (Sigma-Aldrich); and CD45.1 (eBioscience) followed by fluorophore-conjugated secondary antibody. The stained sections were viewed using an Olympus IX 70 fluorescence microscope, and the images were analyzed using ImageJ.

Laser capture microdissection, RNA amplification, and RT-qPCR. Aortic root sections were stained for CD11c or sm-actin as described above. Using these images as a guide, CD11c^{hi}, CD11c^{lo}, and sm-actin$^+$ regions were marked in the next serial section, and those regions were selectively subjected to laser capture using a PALM laser capture microdissection (LCM) machine. RNA was isolated using the RNeasy Micro Kit (Qiagen). Linear amplification of the RNA was performed using the MessageAmp II aRNA Kit (Ambion). The purity of the obtained RNA was estimated by measuring absorbance at 260 and 280 nm using a NanoDrop (Thermo Scientific). RNA with an A260/280 of >1.8 was used for cDNA synthesis. cDNA conversion of the amplified RNA was performed using the SuperScript VILO cDNA Synthesis Kit (Invitrogen). qPCR was performed in an 7500 Real-Time PCR system (Applied Biosystems) using SYBR green chemistry. Specific primers used were as follows: IL-12 p40 (5′-CCTGCATCTAGAGGCTGTCC-3′ / 5′-GGCAAACCAGGAGATGGTTA-3′); TNF-α (5′-CATCTTCT-CAAAATTCGAGTGACAA-3′ / 5′-TGGGAGTAGACAAGGTACAACCC-3′); IFN-γ (5′-GCGTCATTGAATCACACCTG-3′ / 5′-TGAGCTCATTGAAT-GCTTGG-3′); IL-10 (5′-CATGGGTCTTGGGAAGAGAA-3′ / 5′-AACTGGC-CACAGTTTTCAGG-3′); TGF-β (5′-GGACTCTCCACCTGCAAGAC-3′ / 5′-GACTGGCGAGCCTTAGTTTG-3′); IL-2 (5′-AAGCTCTACAGCGGAAG-CAC-3′ / 5′-ATCCTGGGGAGTTTCAGGTT-3′); GATA3 (5′-GTCATCCCT-GAGCCACATCT-3′ / 5′-AGGGCTCTGCCTCTCTAACC-3′); Tbet (5′-GGT-GTCTGGGAAGCTGAGAG-3′ / 5′-GAAGGACAGGAATGGGAACA-3′); FoxP3 (5′-TCTTGCCAAGCTGGAAGACT-3′ / 5′-GGGGGTTCAAG-GAAGAAGAGG-3′); IL-17A (5′-TCTCTGATGCTGTTGCTGCT-3′ / 5′-AGGAAGTCCTTGGCCTCAGT-3′); RORγT (5′-AAGCTGAAGGCAGA-GACAGC-3′ / 5′-TGTTCTGGTTCCCCAAGTTC-3′); CX3CR1 (5′-GGA-GACTGGAGCCAACAGAG-3′ / 5′-CCTGATCCAGGGAATGCTAA-3′); MCP-1 (5′-CCCCACTCACCTGCTGCTACT-3′ / 5′-TTTACGGGTCAACTT-GACATTC-3′); ColA1 (5′-GTTCGGGGCTGATGTACCAGT-3′ / 5′-GAGCG-

from this study may help inform the design of DC-mediated antiatherosclerosis vaccines and other therapeutic strategies that take advantage of the atheroprotective action of Tregs and their cytokines (15, 45, 48, 58, 59).

Methods

Generation of chimeric mice, diets, and lipid analysis. The CD11cCre (stock 008068) and MyD88 floxed mice (stock 008888) were obtained from The Jackson Laboratory on a C57BL/6J background. These 2 strains of mice were bred in the animal facility of Columbia University to generate Cre$^+$ and Cre$^-$ mice. 8-week-old male *Ldlr$^{-/-}$* mice (stock 002207, The Jackson Laboratory) were lethally irradiated (10 Gy), and their bone marrow was reconstituted by transplanting marrow cells isolated from 8-week-old Cre$^-$ or Cre$^+$ mice. 6 weeks after irradiation and bone marrow transplantation, the mice were fed a high-fat, high-cholesterol WD (TD 88137, Harlan Teklad) ad libitum for 10 weeks. At the end of the study, the mice were fasted overnight, weighed, anesthetized using isoflurane, and euthanized. Blood samples were collected from the left ventricle for cellular and lipid analysis. Total plasma cholesterol was measured using the Cholesterol E Kit from Wako, and plasma triglycerides were measured using the L-Type Triglyceride M Color B Kit from Wako. For measurement of the lipoprotein profile, plasma samples were fractionated by fast-performance liquid chromatography on a Superose 6 column at a flow rate of 0.2 ml/min, and the cholesterol content of each fraction was determined using a commercially available kit (Wako). All mouse protocols were approved by the Columbia University Institutional Animal Care and Use Committee.

Aortic root atherosclerotic lesion analysis. After euthanizing each mouse, the heart and the arterial tree were perfused with saline. The aortic root was placed in OCT medium and was immediately frozen. Using a cryomicrotome, sections were cut serially at 8-μm intervals, starting from the aortic sinus, and mounted on slides. For lesion area analysis, the sections were stained with eosin and hematoxylin, and the intimal lesion area was quantified by averaging measurements from 6 sections 50 μm apart using a Nikon Labophot 2 microscope and Image Pro Plus image analysis software.

GAGAGTACTGGATCG-3′) ColA3 (5′-GACCTCGTGCTCCAGTTAGC-3′ / 5′-ACCAAAAGGTGATGCTGGAC-3′); MyD88 (5′-CACCTGTGTCT-GGTCCATT-3′ / 5′-AGGCTGAGTGCAAACTTG-3′); Egr-1 (5′-CCACAA-CAACAGGGAGACCT-3′ / 5′-ACTGAGTGGCGAAGGCTTTA-3′).

Aortic cell preparation and flow cytometry. Aortic single cell preparation was conducted as described previously (60). Briefly, whole aorta was dissected from adjoining tissues, and the adventitial fat was cleaned. The aorta was then dissected and incubated with a digestion buffer containing 125 U/ml collagenase type XI, 60 U/ml hyaluronidase type I-s, 60 U/ml DNase1, and 450 U/ml collagenase type I in PBS containing 20 mM HEPES at 37°C for 1 hour. The released cells were then stained with primary and secondary antibodies and analyzed by flow cytometry. To estimate the efficiency of recovery of leukocytes from the aorta, the *Cd45* mRNA levels were quantified by real-time RT-qPCR of RNA extracted from the released aortic cells versus the residual aortic tissue, and these numbers were then compared with *Cd45* mRNA obtained from known numbers of peripheral blood leukocytes (60). The estimated recovery was >80%.

Fluorescent bead labeling of Ly6C^{hi} monocytes. To track newly recruited monocytes in atherosclerotic lesions, the Ly6C^{hi} subset of monocytes was labeled with fluorescent beads as described previously (23). Briefly, 96 hours before the end of study, the mice were injected i.v. with 250 μl clodronate-containing liposomes (http://clodronateliposomes.org/ash-windigital.asp?docid=26) to deplete monocytes. 48 hours later, the mice were injected with 250 μl of a 1:4 dilution of 1 μm Fluoresbrite Plain YG microspheres (Polysciences). 48 hours after this injection, the mice were euthanized, and peripheral blood samples were analyzed by flow cytometry to quantify the efficiency of bead labeling of Ly6C^{hi} monocytes. The heart and aortic tissues were processed as described above. The newly recruited bead-labeled monocytes in the atherosclerotic lesions were visualized by fluorescence microscopy and quantified using ImageJ.

MCP-1 and TGF-β ELISA assays. ELISA assays for serum MCP-1 and TGF-β were performed using commercially available kits (Mouse CCL2 [MCP-1] ELISA Ready-SET-Go and Human TGF-β1 ELISA Ready-SET-Go [second generation]; eBioscience) as per manufacturer's instructions. For measurement of nascent TGF-β in atherosclerotic lesions, 6 sections per mouse were homogenized in a lysis buffer containing 0.5% Triton X-100, 150 mM NaCl, 15 mM Tris, 1 mM CaCl2, and 1 mM MgCl$_2$, pH 7.4. The homogenates were then treated with 1 N HCl for acid activation of latent TGF-β and then neutralized with 1 N NaOH prior to ELISA per the manufacturer's instructions.

Antibody-mediated depletion of Tregs. Two weeks prior to the end of the study, appropriate groups of mice were injected i.p. with 25 μg anti-CD25 antibody (clone PC61, BD Biosciences) or control IgG antibody (7). The efficiency of Treg depletion was monitored by assaying Treg numbers in the spleen and iliac lymph nodes by flow cytometry.

Adoptive transfer of Tregs. Tregs were isolated from the spleens of 8-week-old CD45.1 C57BL6/J mice by MACS using the CD4$^+$CD25$^+$ Regulatory

T Cell Isolation Kit (Miltenyi Biotech). Two weeks prior to the end of the experiment, 10^6 purified Tregs per mouse were injected i.v. into 8-week WD-fed CD45.2 Cre$^+$ mice. The control mice received an equal volume saline injection. The number of splenic Tregs and CD45.1$^+$ Tregs was determined by flow cytometry.

Immunoneutralization of TGF-β and MCP-1. Cre$^-$ and Cre$^+$ mice were injected i.v. with 100 μg neutralizing anti–MCP-1 or anti–TGF-β antibody (R&D Systems) on days 1, 3, and 8 prior to end of the 10-week WD feeding period. Control mice received IgG antibody.

In vitro Teff cell and Treg generation from naive T cells. Bone marrow cells were isolated from Cre$^-$ and Cre$^+$ mice and differentiated to DCs by culturing them with 10 ng/ml GM-CSF and 10 ng/ml IL-4 for 7 days. These bone marrow–derived DCs were loaded with ova and treated with or without 5 μg CpG to induce DC maturation. Naive T cells (CD44^{lo} CD62L^{hi}) were sorted from splenocytes of OT-II transgenic mice that express a T cell receptor specific for Ova$_{323-339}$ peptide. These naive T cells, which were >95% pure, were coincubated with the ova-loaded DCs at a ratio of 1:5. Certain groups were treated with anti-CD28 antibody (2 μg/ml) to provide exogenous costimulation to T cells. 72 hours later, the cells were harvested and immunostained with fluorophore-conjugated antibodies against CD4, CD44, CD62L, CD25, and FoxP3 and analyzed by flow cytometry.

Statistics. The data displayed are mean ± SEM. The *n* numbers are indicated for each experiment in the figure legends. Comparison of mean values between groups was analyzed using Student's *t* test or Mann-Whitney *U* test. *P* values of less than 0.05 were considered significant.

Address correspondence to: Manikandan Subramanian or Ira Tabas, Columbia University Medical Center, Department of Medicine, 630 West 168th Street, New York, New York 10032, USA. Phone: 212.305.5669; Fax: 212.305.4834; E-mail: ms4144@columbia.edu (M. Subramanian). Phone: 212.305.9430; Fax: 212.305.4834; E-mail: iat1@columbia.edu (I. Tabas).

1. Hansson GK, Hermansson A. The immune system in atherosclerosis. *Nat Immunol.* 2011;12(3):204–212.
2. Members WG, et al. Heart Disease and Stroke Statistics—2012 Update. *Circulation.* 2012;125(1):e2–e220.
3. Tacke F, et al. Monocyte subsets differentially employ CCR2, CCR5, and CX3CR1 to accumulate within atherosclerotic plaques. *J Clin Invest.* 2007;117(1):185–194.
4. Trinchieri G. Interleukin-12: A proinflammatory cytokine with immunoregulatory functions that bridge innate resistance and antigen-specific adaptive immunity. *Annu Rev Immunol.* 1995;13:251–276.
5. Mallat Z, Taleb S, Ait-Oufella H, Tedgui A. The role of adaptive T cell immunity in atherosclerosis. *J Lipid Res.* 2009;50(suppl):S364–S369.
6. Buono C, Binder CJ, Stavrakis G, Witztum JL, Glimcher LH, Lichtman AH. T-bet deficiency reduces atherosclerosis and alters plaque antigen-specific immune responses. *Proc Natl Acad Sci U S A.* 2005;102(5):1596–1601.
7. Ait-Oufella H, et al. Natural regulatory T cells control the development of atherosclerosis in mice. *Nat Med.* 2006;12(2):178–180.
8. Butcher MJ, Gjurich BN, Phillips T, Galkina EV. The IL-17A/IL-17RA axis plays a proatherogenic role via the regulation of aortic myeloid cell recruitment / novelty and significance. *Circ Res.* 2012;110(5):675–687.
9. Taleb S, et al. Loss of SOCS3 expression in T cells reveals a regulatory role for interleukin-17 in atherosclerosis. *J Exp Med.* 2009;206(10):2067–2077.
10. Gautier EL, et al. Conventional dendritic cells at the crossroads between immunity and cholesterol homeostasis in atherosclerosis. *Circulation.* 2009;119(17):2367–2375.
11. Shaposhnik Z, Wang X, Weinstein M, Bennett BJ, Lusis AJ. Granulocyte macrophage colony-stimulating factor regulates dendritic cell content of atherosclerotic lesions. *Arterioscler Thromb Vasc Biol.* 2007;27(3):621–627.
12. Sun J, et al. Deficiency of antigen-presenting cell invariant chain reduces atherosclerosis in mice. *Circulation.* 2010;122(8):808–820.
13. MacRitchie N, et al. Plasmacytoid dendritic cells play a key role in promoting atherosclerosis in apolipoprotein e-deficient mice. *Arterioscler Thromb Vasc Biol.* 2012;32(11):2569–2579.
14. Choi J-H, et al. Flt3 Signaling-dependent dendritic

cells protect against atherosclerosis. *Immunity*. 2011;35(5):819–831.

15. Hermansson A, Johansson DK, Ketelhuth DFJ, Andersson J, Zhou X, Hansson GK. Immunotherapy with tolerogenic apolipoprotein B-100-loaded dendritic cells attenuates atherosclerosis in hypercholesterolemic mice. *Circulation*. 2011;123(10):1083–1091.

16. Klingenberg R, et al. Intranasal immunization with an apolipoprotein B-100 fusion protein induces antigen-specific regulatory T cells and reduces atherosclerosis. *Arterioscler Thromb Vasc Biol*. 2010;30(5):946–952.

17. Hou B, Reizis B, DeFranco AL. Toll-like receptors activate innate and adaptive immunity by using dendritic cell-intrinsic and -extrinsic mechanisms. *Immunity*. 2008;29(2):272–282.

18. Packard R, Lichtman A, Libby P. Innate and adaptive immunity in atherosclerosis. *Semin Immunopathol*. 2009;31(1):5–22.

19. Koltsova EK, et al. Dynamic T cell–APC interactions sustain chronic inflammation in atherosclerosis. *J Clin Invest*. 2012;122(9):3114–3126.

20. Paulson KE, Zhu S-N, Chen M, Nurmohamed S, Jongstra-Bilen J, Cybulsky MI. Resident intimal dendritic cells accumulate lipid and contribute to the initiation of atherosclerosis. *Circ Res*. 2010;106(2):383–390.

21. Liu P, et al. CX3CR1 deficiency impairs dendritic cell accumulation in arterial intima and reduces atherosclerotic burden. *Arterioscler Thromb Vasc Biol*. 2008;28(2):243–250.

22. Weber C, et al. CCL17-expressing dendritic cells drive atherosclerosis by restraining regulatory T cell homeostasis in mice. *J Clin Invest*. 2011;121(7):2898–2910.

23. Potteaux S, et al. Suppressed monocyte recruitment drives macrophage removal from atherosclerotic plaques of Apoe−/− mice during disease regression. *J Clin Invest*. 2011;121(5):2025–2036.

24. Saederup N, Chan L, Lira SA, Charo IF. Fractalkine deficiency markedly reduces macrophage accumulation and atherosclerotic lesion formation in CCR2−/− mice. *Circulation*. 2008;117(13):1642–1648.

25. Shevach EM. Mechanisms of Foxp3+ T regulatory cell-mediated suppression. *Immunity*. 2009;30(5):636–645.

26. Stephens LA, Gray D, Anderton SM. CD4+CD25+ regulatory T cells limit the risk of autoimmune disease arising from T cell receptor crossreactivity. *Proc Natl Acad Sci U S A*. 2005;102(48):17418–17423.

27. Mottet C, Uhlig HH, Powrie F. Cutting edge: cure of colitis by CD4+CD25+ regulatory T cells. *J Immunol*. 2003;170(8):3939–3943.

28. Kitamura M. Identification of an inhibitor targeting macrophage production of monocyte chemoattractant protein-1 as TGF-beta 1. *J Immunol*. 1997;159(3):1404–1411.

29. Feinberg MW, et al. Essential role for Smad3 in regulating MCP-1 expression and vascular inflamma-tion. *Circ Res*. 2004;94(5):601–608.

30. ten Dijke P, Arthur HM. Extracellular control of TGF[beta] signalling in vascular development and disease. *Nat Rev Mol Cell Biol*. 2007;8(11):857–869.

31. Ménoret A, Myers LM, Lee S-J, Mittler RS, Rossi RJ, Vella AT. TGFβ protein processing and activity through TCR triggering of primary CD8+ T regulatory cells. *J Immunol*. 2006;177(9):6091–6097.

32. Yilmaz A, et al. Emergence of dendritic cells in rupture-prone regions of vulnerable carotid plaques. *Atherosclerosis*. 2004;176(1):101–110.

33. Bobryshev YV, Lord RS. Ultrastructural recognition of cells with dendritic cell morphology in human aortic intima. Contacting interactions of vascular dendritic cells in athero-resistant and athero-prone areas of the normal aorta. *Arch Histol Cytol*. 1995;58(3):307–322.

34. Bobryshev YV, Lord RS. S-100 positive cells in human arterial intima and in atherosclerotic lesions. *Cardiovasc Res*. 1995;29(5):689–696.

35. Jongstra-Bilen J, Haidari M, Zhu S-N, Chen M, Guha D, Cybulsky MI. Low-grade chronic inflammation in regions of the normal mouse arterial intima predisposed to atherosclerosis. *J Exp Med*. 2006;203(9):2073–2083.

36. Luchtefeld M, et al. Chemokine receptor 7 knock-out attenuates atherosclerotic plaque development. *Circulation*. 2010;122(16):1621–1628.

37. Hamilton JA. GM-CSF in inflammation and autoimmunity. *Trends Immunol*. 2002;23(8):403–408.

38. Bjorkbacka H, et al. Reduced atherosclerosis in MyD88-null mice links elevated serum cholesterol levels to activation of innate immunity signaling pathways. *Nat Med*. 2004;10(4):416–421.

39. Michelsen KS, et al. Lack of Toll-like receptor 4 or myeloid differentiation factor 88 reduces atherosclerosis and alters plaque phenotype in mice deficient in apolipoprotein E. *Proc Natl Acad Sci U S A*. 2004;101(29):10679–10684.

40. van den Berg TK, Kraal G. A function for the macrophage F4/80 molecule in tolerance induction. *Trends Immunol*. 2005;26(10):506–509.

41. Geissmann F, Gordon S, Hume DA, Mowat AM, Randolph GJ. Unravelling mononuclear phagocyte heterogeneity. *Nat Rev Immunol*. 2010;10(6):453–460.

42. Cho HJ, et al. Induction of dendritic cell-like phenotype in macrophages during foam cell formation. *Physiol Genomics*. 2007;29(2):149–160.

43. Thorp E, Cui D, Schrijvers DM, Kuriakose G, Tabas I. Mertk receptor mutation reduces efferocytosis efficiency and promotes apoptotic cell accumulation and plaque necrosis in atherosclerotic lesions of Apoe−/− mice. *Arterioscler Thromb Vasc Biol*. 2008;28(8):1421–1428.

44. Seitz HM, Camenisch TD, Lemke G, Earp HS, Matsushima GK. Macrophages and dendritic cells use different Axl/Mertk/Tyro3 receptors in clearance of apoptotic cells. *J Immunol*. 2007;178(9):5635–5642.

45. van Puijvelde GHM, et al. Induction of oral roler-ance to HSP60 or an HSP60-Peptide activates T cell regulation and reduces atherosclerosis. *Arterioscler Thromb Vasc Biol*. 2007;27(12):2677–2683.

46. Yang K, Li D, Luo M, Hu Y. Generation of HSP60-specific regulatory T cell and effect on atherosclerosis. *Cell Immunol*. 2006;243(2):90–95.

47. Gotsman I, et al. Impaired regulatory T-cell response and enhanced atherosclerosis in the absence of inducible costimulatory molecule. *Circulation*. 2006;114(19):2047–2055.

48. Li H, Ding Y, Yi G, Zeng Q, Yang W. Establishment of nasal tolerance to heat shock protein-60 alleviates atherosclerosis by inducing TGF-β-dependent regulatory T cells. *J Huazhong Univ Sci Technolog Med Sci*. 2012;32(1):24–30.

49. Sakaguchi S, Wing K, Onishi Y, Prieto-Martin P, Yamaguchi T. Regulatory T cells: how do they suppress immune responses? *Int Immunol*. 2009;21(10):1105–1111.

50. Takahashi T, et al. Immunologic self-tolerance maintained by CD25+CD4+ naturally anergic and suppressive T cells: induction of autoimmune disease by breaking their anergic/suppressive state. *Int Immunol*. 1998;10(12):1969–1980.

51. Curotto de Lafaille MA, Lafaille JJ. Natural and adaptive Foxp3+ regulatory T cells: more of the same or a division of labor? *Immunity*. 2009;30(5):626–635.

52. Gotsman I, Gupta R, Lichtman AH. The influence of the regulatory T lymphocytes on atherosclerosis. *Arterioscler Thromb Vasc Biol*. 2007;27(12):2493–2495.

53. Maganto-García E, et al. Foxp3+-inducible regulatory t cells suppress endothelial activation and leukocyte recruitment. *J Immunol*. 2011;187(7):3521–3529.

54. Lievens D, et al. Abrogated transforming growth factor beta receptor II (TGFβRII) signalling in dendritic cells promotes immune reactivity of T cells resulting in enhanced atherosclerosis [published online ahead of print May 21, 2012]. *Eur Heart J*. doi:10.1093/eurheartj/ehs106.

55. Mallat Z, et al. Protective role of interleukin-10 in atherosclerosis. *Circ Res*. 1999;85(8):e17–e24.

56. Virmani R, Burke AP, Farb A, Kolodgie FD. Pathology of the vulnerable plaque. *J Am Coll Cardiol*. 2006;47(8 suppl):C13–C18.

57. Mallat Z, et al. Inhibition of transforming growth factor-β signaling accelerates atherosclerosis and induces an unstable plaque phenotype in mice. *Circ Res*. 2001;89(10):930–934.

58. Habets KL, et al. Vaccination using oxidized low-density lipoprotein-pulsed dendritic cells reduces atherosclerosis in LDL receptor-deficient mice. *Cardiovasc Res*. 2010;85(3):622–630.

59. Hansson G, Nilsson J. Vaccination against atherosclerosis? Induction of atheroprotective immunity. *Semin Immunopathol*. 2009;31(1):95–101.

60. Galkina E, Kadl A, Sanders J, Varughese D, Sarembock IJ, Ley K. Lymphocyte recruitment into the aortic wall before and during development of atherosclerosis is partially L-selectin dependent. *J Exp Med*. 2006;203(5):1273–1282.